

Progress Report to the Department of Energy  
**Thermodynamic and Kinetic Aspects of Surface Acidity**

DE-FG01-84ER13183

DOE/ER/13183--T1

James A. Dumesic

DE92 011194

University of Wisconsin-Madison

## I. Introduction

Our research funded by the Department of Energy in the general area of acid catalysis involves 1) the characterization of solid acidity, 2) the assessment of catalytic performance of acidic materials, and 3) the elucidation of possible relationships between surface thermodynamic and kinetic properties of acidic sites. During the past year we have focused on zeolitic acid catalysts and on methylamine synthesis from ammonia and methanol. Part of our work has also involved elucidation of the role of acidity in the selective catalytic reduction of nitric oxide over vanadia/titania.

Acidic zeolites find use in a wide variety of catalytic applications, ranging from large scale petrochemical processes to the synthesis of specialty chemicals. Quantitative characterization of catalyst acid properties is important for elucidation of the role of surface acidity in determining the catalytic activity and selectivity of these materials. However, solid acid catalysts have long posed a challenge for quantitative characterization. Accordingly, one aspect of our research addresses the problem of quantitative characterization of zeolite acidity.

Dehydrative methylamine synthesis from ammonia and methanol is an important example of an acid catalyzed reaction for specialty chemicals production. Amines are used in a number of applications such as pharmaceuticals, herbicides, pesticides, solvents, surfactants and detergents [1]. Production of methylamines in the U.S. is approximately 270 Mlb per year [2]. In addition to this commercial importance, the methylamine synthesis reaction is of scientific interest; it poses the classic problem of series selectivity combined with adsorption and readsorption phenomena for each intermediate species. An understanding of the mechanistic details of such a reaction would be of general interest and utility.

The objectives of our acid characterization work are based in determining 1) the type of acid site, 2) the strength of the sites, 3) the number of sites of different strength, and 4) the mobility of molecules adsorbed on the acid sites. An accurate measure of acid strength is given by the heat of adsorption of a basic probe molecule on the acid site,  $\Delta H_{ads}$ . In general, a catalyst may have sites of different strength and there will thus be a distribution of numbers of sites in strength. The mobility of a molecule adsorbed on an acid site is also an important probe of the site. A thermodynamic representation of this mobility is given by

MASTER

Co

(Con't Notice of Energy RD&D Project)

6. Descriptive Summary (limit to 200 words)

Our research in the general area of acid catalysis involves the characterization of solid acidity and the corresponding assessment of catalytic performance of acidic materials. Acid characterization studies are required to provide essential information about the type of acid site (i.e., Lewis versus Bronsted), the strength of the sites, and the mobility of molecules adsorbed on the acid sites. An accurate measure of acid strength is given by the heat of adsorption of a basic probe molecule on the acid site. A thermodynamic representation of the mobility of adsorbed species on these sites is given by the entropy of adsorption. Important techniques used in these acid site characterization studies include microcalorimetry, thermogravimetric measurements, temperature programmed desorption, infrared spectroscopy and solid state nuclear magnetic resonance. The combination of these acid site characterization studies with reaction kinetics measurements of selected catalytic processes allows the elucidation of possible relationships between surface thermodynamic and kinetic properties of acidic sites. Such relationships are important milestones in formulating effective strategies for the effective utilization of solid acid catalysts. Current work in this direction involves methylamine syntheses over various zeolites, and the basic probe molecules employed include ammonia, methanol, water and mono-, di- and tri-methylamines.

## DISCLAIMER

This report was prepared as an account of work sponsored by an agency of the United States Government. Neither the United States Government nor any agency thereof, nor any of their employees, makes any warranty, express or implied, or assumes any legal liability or responsibility for the accuracy, completeness, or usefulness of any information, apparatus, product, or process disclosed, or represents that its use would not infringe privately owned rights. Reference herein to any specific commercial product, process, or service by trade name, trademark, manufacturer, or otherwise does not necessarily constitute or imply its endorsement, recommendation, or favoring by the United States Government or any agency thereof. The views and opinions of authors expressed herein do not necessarily state or reflect those of the United States Government or any agency thereof.

the entropy of adsorption,  $\Delta S_{\text{ads}}$ . Acid site type refers to Brønsted (proton donating) or Lewis (electron pair accepting) classifications.

Upon developing methods of determining these features on a quantitative basis, it is of importance to measure acidity for a wide variety of materials encompassing different structure, composition and pretreatment. This work would accomplish the further objective of determining the effect of various modifications on zeolite acidity, and provide a basis set of catalysts with which to perform kinetic studies.

The objectives of our reaction kinetics studies are to determine first the catalytic behavior of characterized materials and second to relate the catalytic behavior to quantified acidity features. This task entails measurements of selectivity, activity, kinetic orders and activation energy, all of which are likely to be influenced by the acidity features of a particular catalyst. These reaction characteristics and the manner in which they are related to solid acidity yield valuable reaction mechanistic information.

Another important aspect of our work is the evaluation of thermodynamic quantities related to methylamine synthesis, since these quantities may be used to probe the energetics of available reaction pathways. Specifically, this effort is in the measurement of heats and entropies of adsorption for the reactants and products of the methylamine synthesis reaction. Combined with detailed kinetic measurements, these measurements may yield relationships between thermodynamic and kinetic properties. Such relationships would be important milestones in formulating effective strategies for the effective utilization of solid acid catalysts.

The method by which these objectives are to be achieved employs multiple experimental techniques. For the characterization studies, infrared spectroscopy, microcalorimetry, temperature programmed desorption (TPD), thermogravimetric analysis and <sup>2</sup>D NMR are being used. Kinetic measurements are made in a flow-through apparatus operating at ambient pressure. Measurements of the heats and entropies of adsorption for various reaction species are made using microcalorimetry.

Finally, our studies of the role of acidity in the selective catalytic reduction of nitric oxide over vanadia/titania have employed temperature programmed desorption of ammonia from 1) low surface area materials under vacuum condition and 2) high surface area catalysts under flow conditions. Temperature programmed reaction studies of nitric oxide with preadsorbed ammonia were conducted to probe the catalytic properties of the acid sites.

## II Characterization Studies

### A. Catalysts Studied

The results of our recent characterization studies are described below. The first set of catalysts studied were a set of zeolites, free of chemical, hydrothermal, or high temperature (above 723K) treatment, including: H-ZSM-5 (Si/Al = 34), H-mordenite (Si/Al = 13) and H-Y zeolite (Si/Al = 2.4). These catalysts were studied by microcalorimetry, thermogravimetry, temperature programmed desorption and infrared spectroscopy. A second set of catalysts was used to study the effect of various modifications on zeolite acidity, namely: 1)  $\text{Na}^+$  level on H-Y zeolite, 2)  $\text{K}^+$  level on H-ZSM-5, 3) high temperature calcination on H-mordenite, and 4) steaming on FCC catalysts.

### B. Results of Characterization Studies for H-ZSM-5, H-Mordenite and H-Y Zeolite

#### 1. Microcalorimetric Results for H-ZSM-5, H-Mordenite and H-Y Zeolite

The differential heat of adsorption of pyridine obtained by microcalorimetry on H-ZSM-5 is shown in Figure 1 as a function of coverage. An important aspect of this curve is that it shows a large number of sites of nearly constant strength, *i.e.*, near 160 kJ/mol for pyridine adsorption. Infrared spectroscopy was used to confirm that these sites are Brønsted acid centers. There is also evidence for strong sites, evidenced by the initially high differential heats, which may be associated with non-framework aluminum species. At higher coverages, weaker adsorption sites near about 100 kJ/mol are filled. This weaker interaction is of the same strength as for pyridine adsorption on silica, which can be characterized as resulting from hydrogen bonding.

The same general features described above are found for the differential heat of pyridine adsorption on H-mordenite, as shown in Figure 2. A large number of sites with nearly constant strength is observed on H-mordenite near 200 kJ/mol, this value being about 40 kJ/mol stronger than those sites of H-ZSM-5. There is also evidence for a small number of sites stronger than 200 kJ/mol, as well as weak sites near 110 kJ/mol. The total number of sites is larger for H-mordenite compared to H-ZSM-5, as expected from the higher aluminum content on this zeolite.

In contrast to the previous two samples, H-Y zeolite shows Brønsted acid sites of varying strength, as shown by the multiple plateaus in the differential heat curve of Figure 3. These plateaus are representative of acid sites with strengths near 180, 150 and 130 kJ/mol; there is also a small number of sites with strengths higher than 200 kJ/mol for pyridine adsorption. This fundamental difference between the acid strength distribution of H-Y zeolite

compared to H-ZSM-5 and H-mordenite, namely a wider distribution of Brønsted site strengths for H-Y zeolite, may be related to the higher aluminum content of this sample. It should be noted that the total pyridine coverage for this sample is about half of that value expected from Si/Al ratio, and this result is probably related to the fact that a fraction of the framework hydroxyl groups are inaccessible to pyridine adsorption because of their location in the lattice [3].

## 2. Thermogravimetric Results for H-ZSM-5, H-Mordenite and H-Y Zeolite

Pyridine adsorption isotherms at 473 and 673 K were obtained gravimetrically for the above three samples. Figure 4 shows representative adsorption isotherms for H-Y zeolite. An important feature of these gravimetric experiments is that adsorption at high temperatures (673 K) has been employed, whereas microcalorimetric adsorption studies were conducted at the lower temperature of 473 K. Since adsorption-desorption equilibrium between pyridine on the strongest sites and pyridine in the gas phase is not attained at the lower temperature of 473 K, surface diffusion is the mechanism by which the strongest sites may be selectively titrated during sequential exposure of the sample to pyridine [4]. Upon increasing the adsorption temperature to 673 K, adsorption-desorption equilibrium between adsorbed and gas phase pyridine can be more nearly achieved, thus allowing equilibrium isotherms to be approached.

The gravimetric determinations of the saturation coverages of pyridine at 473 K are in good agreement with the microcalorimetric results. At 673 K, pyridine adsorption occurs almost exclusively on sites stronger than about 120 kJ/mol, whereas pyridine adsorption at 473 K is effective for titration of essentially all acid sites. Combinations of adsorption isotherms have been used to fit the gravimetric data, also shown in Figure 4. The adsorption equilibrium constants from this fitting procedure were then used with the heat of adsorption data from microcalorimetry to estimate entropies of adsorption. This procedure was performed for the above zeolites, as well as for an amorphous silica-alumina sample and a commercial FCC catalyst (Engelhard). A plot of the heat of adsorption for the Brønsted acid sites against the entropies of adsorption for these sites is shown in Figure 5. There is a clear relationship between the strength of the adsorption site and the entropy change for pyridine adsorption on the site. A similar trend has been found previously for hydrocarbon adsorption on X and Y zeolites [5].

## 3. TPD for H-ZSM-5 and H-Mordenite

Figure 6 shows the temperature programmed desorption curve of pyridine from H-ZSM-5. The two peaks are consistent with adsorption sites of two different strengths. The larger area for the higher temperature peak indicates that acid sites of this strength predominate

on the sample, in agreement with the microcalorimetry results. The results of computer simulation of the H-ZSM-5 desorption spectrum using the values of  $\Delta H_{\text{ads}}$ ,  $\Delta S_{\text{ads}}$ , and number of sites from the gravimetry and microcalorimetry results are also shown in the Figure 6. The agreement in the peak temperature is satisfactory, considering that no adjustable parameters were used. The shape of the simulated desorption curve is significantly narrower than that measured by experiment. This behavior may be due to readsorption on the walls of the apparatus before the pyridine reaches the detector, since we have shown that heating of the TPD apparatus walls results in narrower desorption peaks. Current experiments are being conducted with heating of the walls so as to narrow the desorption peak.

Figure 7 shows the TPD curve for pyridine desorption from H-mordenite. In this case there is a somewhat larger number of the weaker sites as well as a broadening of the high temperature peak. Since readsorption is significant, it is not possible to compare directly the peak temperatures of the H-ZSM-5 and H-mordenite; however, given the similar number of sites in both samples and the constant heating rate, the higher peak temperature for H-mordenite is consistent with the stronger acid sites measured by microcalorimetry. The simulation using the gravimetric and microcalorimetric measurements also shows good agreement.

#### **4. Infrared Spectroscopy Results for H-Y Zeolite.**

Infrared spectra of adsorbed pyridine yield measurements of Lewis and Brønsted acid site populations via characteristic absorption bands of pyridine adsorbed on each site type. Studies of the H-ZSM-5 and H-mordenite reveal that Brønsted sites predominate for these samples. More detailed infrared spectroscopic studies of H-Y zeolite were conducted so as to determine the nature of the acid sites giving rise to the various plateaus in the acid strength distribution for this catalyst.

Pyridine was dosed onto the surface of H-Y zeolite to obtain coverages corresponding to 100, 300, 600, 1000, and 1800  $\mu\text{mol/g}$ . Infrared spectra were obtained at increasing coverages, as shown in Figure 8. These results demonstrate that Brønsted acid sites are selectively populated by pyridine until relatively high coverages (about 1000  $\mu\text{mol/g}$ ), whereupon Lewis acid sites are occupied. In combination with the microcalorimetric results, this behavior indicates that Brønsted acid sites vary widely in strength, and that the Lewis sites of H-Y zeolite are relatively weak in acid strength.

#### **5. Deuterium NMR Studies of Brønsted Acidity**

Our studies of zeolite acidity have recently utilized deuterium NMR to probe the environment of Brønsted acid sites. In particular,  $^2\text{D}$  is a quadrupolar nucleus and the quadrupole coupling constant, QCC, provides a

useful measure of the electric field gradient at the deuterium nucleus. The initial goal of these studies was to determine the feasibility of this approach in distinguishing different types of Brønsted acid sites in various zeolites, *i.e.*, Y-zeolite, ZSM-5 and mordenite. We first demonstrated that high quality  $^2\text{D}$  NMR spectra can, in fact, be obtained after exchanging the protons with deuterons in sample treatments with  $\text{D}_2\text{O}$ . These treatments, however, are not selective, since exchange is observed to take place with acidic, as well as non-acidic, hydrogen in the catalyst. In particular, the  $^2\text{D}$  NMR spectra subsequently collected show two Pake doublets due to acidic deuterons and a Gaussian component due to non-acidic deuterons, *e.g.*, silanol groups. Exposure of the samples to  $\text{NH}_3$  shows preferential interaction with the Brønsted acid sites, and moreover, the deuterons having the larger QCC appear to be stronger acid sites.

Following our initial  $^2\text{D}$  NMR studies, we conducted more detailed studies employing toluene- $d_8$  to exchange the protons in the sample with deuterium. This approach was shown to lead to selective exchange of the acidic sites, thereby simplifying interpretation of the subsequent  $^2\text{D}$  NMR spectra. Our studies of Y-zeolite, ZSM-5 and mordenite showed that all three zeolites possessed deuterons in at least several different environments. Small doses of pyridine were used to selectively block the strongest acid sites prior to exchange of the remaining sites with toluene- $d_8$ , from which it was shown that deuterons with larger QCC are generally more acidic. We are currently in the process of interpreting these fascinating data in greater detail. The important conclusion from our work to date is that 2D NMR is a method with potential to provide information about the local environment of Brønsted acid sites, thereby allow us to study how the structure of the site controls its acid strength and catalytic properties.

### C. Discussion of Results for H-ZSM-5, H-Mordenite and H-Y Zeolite

The microcalorimetric results on the various zeolites show several important features. The first result is that the H-ZSM-5 and H-mordenite samples have acid sites which are homogeneous in strength, with H-mordenite having the stronger sites. In contrast, H-Y zeolite has sites of varying strength. One possible explanation for the heterogeneity in acid strength distribution for H-Y zeolite is that this sample has a lower Si/Al ratio (equal to 2.4). Evidence in the literature suggests that isolated Al framework atoms (having no next-nearest Al neighbors) have the highest strength and that as the number of next-nearest Al atoms increases, the acid strength is likely to decrease [6-9]. Studies of aluminum distribution in Y zeolite suggest that there may be four different acid strengths corresponding to aluminum atoms with 0, 1, 2, or 3 Al nearest neighbors [10-13]. For a Si/Al ratio equal to 2.4, these studies indicate a small number of isolated Al atoms relative to those with 1 or 2 next-nearest Al neighbors. Thus, the sites of varying strength in H-Y zeolite may be a reflection of aluminum topology, *i.e.* the number

of next-nearest neighbor or more distant Al atoms. The H-mordenite and H-ZSM-5 samples, with their lower aluminum contents, may have fewer interactions of this type, isolated Al atoms comprising the majority of the acid sites.

A quantitative rationalization of acid site strengths is not possible at present; however, it is clear that the heat of adsorption is comprised of at least two contributions [14]. The major factor is the inherent proton-donating ability of the acid site, *i.e.*, the enthalpy of the interaction between the proton and the base. A second factor is the stabilization energy associated with the molecule inside the zeolite lattice and subject to van der Waals interactions. The microcalorimetric measurement of the heat of adsorption of a given molecule contains contributions from both of these factors. Based purely on the aluminum content of the zeolites, it is somewhat surprising that H-mordenite has stronger acid sites than those of H-ZSM-5. However, adsorption studies of hydrocarbons suggest that the electrostatic fields of different zeolite systems can significantly alter the measured heat of adsorption; these differences can range up to 40 kJ/mol depending on the hydrocarbon adsorbed [15,16].

The entropy of adsorption of a molecule on an acidic catalyst is similarly a measure of two factors. As a molecule adsorbs from the gas phase onto an acid site, there is a partial loss of translational and perhaps also rotational degrees of freedom. The entropy of an adsorbed molecule is also a direct reflection of the mobility of this molecule, as influenced by the steric environment around the acid site. The acid site may be configured such that certain motions are inhibited or the distance between sites may be so great as to limit migration of the adsorbate between acid sites.

The relationship between entropy and heat of adsorption is shown in Figure 5. As expected, the stronger the interaction between the acid site and adsorbed molecule, the lower is the mobility of the adsorbed molecule. The fact that the relationship is not strictly linear may reflect the effect of varying catalyst morphology on the entropy of adsorption. As more zeolites are studied, the influence of zeolitic framework on entropy of adsorption may be clarified.

Several general comments can be made about acid catalyst characterization from these studies of various acidic zeolites. In our work, microcalorimetry has been used to provide information about the number and the strength of adsorption sites. Gravimetric measurements have been used to complement these microcalorimetric acid strength measurements and to provide adsorption isotherms. The entropy of adsorption has then been estimated from the adsorption equilibrium constants obtained from fits of adsorption isotherms to the gravimetric data and from the heat of adsorption data obtained microcalorimetrically. Finally, infrared spectroscopy of adsorbed pyridine has been used to distinguish Brønsted from Lewis acid sites.

The slate of techniques used in this study is not unique, but the idea of using multiple techniques to gather information about the various acidity features is paramount. The approach highlighted here is not limited to simple catalyst systems. Recent work on FCC catalysts modified by steam treatment has demonstrated that these techniques [17] as well as temperature programmed desorption of 2-propanamine [18] can be used to examine quantitatively industrial catalysts with complex acidity features.

It is apparent from the above results that the combination of microcalorimetric and thermogravimetric measurements can be used to assess quantitatively the values of  $\Delta H_{ads}$  and  $\Delta S_{ads}$  for the adsorption of basic molecules on acid sites. These measurements, however, require long times during data collection to insure adequate equilibration of the base molecule with the acid sites. Therefore, it would be desirable to develop correlations that would allow surface thermodynamic measurements from a more rapid technique, such as temperature programmed desorption.

Temperature programmed desorption spectra of basic molecules from acidic catalysts, collected in the regime where re-adsorption is fast, provide information about the equilibrium constant for adsorption of the basic probe molecule. The value of  $\Delta G_{ads}$  determined in this manner can then be separated into contributions from  $\Delta H_{ads}$  and  $\Delta S_{ads}$ , provided that a correlation between these two latter values can be established. As demonstrated in Figure 5, such a correlation may, in fact, exist for pyridine adsorption on the Brønsted sites of the catalysts used in this study. The scatter of the data from a simple linear relationship may be associated with the different zeolite morphologies and thus acid site environments. As a first approximation, however, the linear relationship would give a first estimate of the relationship between  $\Delta H_{ads}$  and  $\Delta S_{ads}$ , allowing estimation of these values from TPD spectra. Clearly, these estimates of  $\Delta H_{ads}$  and  $\Delta S_{ads}$  are dependent on the reliability of the relationship between these values. Accordingly, better estimates of these values could be obtained by first using microcalorimetry and thermogravimetric analysis to develop a specific correlation between  $\Delta H_{ads}$  and  $\Delta S_{ads}$  for a family of catalysts and then using this correlation to extract values of  $\Delta H_{ads}$  and  $\Delta S_{ads}$  from TPD spectra of related catalysts.

#### D. Microcalorimetric Results for Modified Zeolites

To determine the effect of various modifications on solid acid features, four series of zeolites were prepared and studied using microcalorimetry. These samples consisted of catalysts for study of the following effects: 1) three H-Y zeolites for  $Na^+$  level, 2) two H-ZSM-5 zeolites for  $K^+$  level, 3) two H-mordenites for high temperature calcination, and 4) four H-Y based FCC catalysts for steaming.

The effect of proton exchange level on H-Y zeolite has been the subject of numerous studies [19-22]. Generally, an increase in acidity with increasing proton exchange has been measured; however, uncertainty exists as to the strength of the acid sites introduced at different exchange levels. Figure 9 shows the differential heat curves for pyridine adsorption on NaHY zeolite with Na<sup>+</sup> contents of 2.24%, 4.31%, and 8.3% (84%, 68%, and 39% levels of proton exchange, respectively). It can be seen that upon decreasing the sodium content from 4.31% to 2.24%, the last sites to be proton exchanged are rather weak, around 130 kJ/mol. Decreasing the Na level from 8.3% to 4.31% results in fairly uniform generation of acid sites with strengths above 110 kJ/mol.

The addition of K<sup>+</sup> to H-ZSM-5 also shows an effect in the reduction of acid strength. Figure 10 shows the differential heat curves obtained by microcalorimetry for an H-ZSM-5 zeolite without K<sup>+</sup> and the same zeolite with 260  $\mu$ mol/g of K<sup>+</sup>. This result demonstrates that there is a reduction in the number of strong acid sites (140 kJ/mol for pyridine adsorption), and that the conversion of strong to weak sites is at approximately a 1:1 ratio. Variation in K<sup>+</sup> level has a dramatic effect on the ratio of strong to weak sites.

Figure 11 demonstrates the effect of calcination at 1010 K on the acidity of H-mordenite. This treatment causes a significant reduction in the total number and the strength of the acid sites. The plateau characteristic of a large number of sites of uniform strength has also disappeared. High temperature calcination is known to induce dealumination and dehydroxylation, both of which are expected to reduce the number of acid sites [23, 24].

The effect of steaming on the number and strength of acid sites of USY FCC catalysts is apparent from comparison of the differential heat curves for the zeolites, shown in Figure 12. There is a sharp decrease in total acidity after just 0.25 h of steaming at 1060 K. The initial heats of pyridine adsorption, corresponding to the strength of the strongest acid sites, decrease with increasing time of steaming from about 200 kJ/mol for the calcined sample to about 170 kJ/mol for the sample steamed for 15 h. However, the most highly steamed sample (steaming for 60 h) shows an initial heat similar to the calcined sample. The microcalorimetric curves also show that the strength of sites comprising the intermediate plateau region progressively decreases with steaming severity.

#### **E. Discussion of Experimental Results for Modified Zeolites**

The studies of modified zeolites reported here demonstrate that there are several means of modifying the strength and number of acid sites and that these changes can be monitored quantitatively. In particular, increasing level of proton exchange results first in a fairly uniform increase in the number of acid sites with strength above 110 kJ/mol. The last sites to be generated have strengths near

130 kJ/mol. The addition of  $K^+$  has a similar effect on the acidity of H-ZSM-5, with a 1:1 correspondence between  $K^+$  level and the conversion of strong to weak sites. High temperature calcination is a well-known method of reducing total acidity via dehydroxylation and dealumination. Infrared spectroscopic studies of these samples show a much higher population of Lewis acid sites on the calcined sample, while the microcalorimetric results shown for H-mordenite give a quantitative assessment of the changes in acid site strength.

### **III. Kinetic Studies of Methylamine Synthesis**

#### **A. Introduction**

Our kinetic studies to date have focused on catalysts which have been characterized via the multi-technique approach described in the previous section. Preliminary work has involved obtaining activation energies and reaction orders in ammonia and methanol at low conversion levels. These studies give information about the initial steps of the reaction to form the primary mono-methylamine product. The main goal of these studies, as mentioned earlier, is to relate the catalyst acidity to catalytic behavior. At the current time, literature studies have primarily emphasized high conversion selectivity [25-29]. Previous kinetic studies have indicated that the reaction proceeds stepwise, with formation of mono-, di- and tri-methylamine occurring in sequence [30,31].

#### **B. General Reaction Characteristics**

A first characteristic of the reaction for all catalysts is that mono-methylamine is formed before di-, or tri-methylamine, in accordance with the previous literature results. An interesting feature of the reaction is that the methylamine product molecules are produced and desorb at relatively low reaction temperatures, even for catalysts which show high acid strength. An important mechanism for desorption of the methylamines may be surface diffusion to the weaker acid sites (at 90-100 kJ/mol for pyridine adsorption) which are present on all catalysts.

Comparison of the turnover frequencies (based on total acid site densities) over the different catalysts shows that there are no wide variations in activity, as shown in Table 1. Even amorphous silica-alumina shows comparable activity; this result suggests that initiation of the reaction is not as demanding of acid site configuration as are hydrocarbon reactions such as catalytic cracking.

#### **C. Activation Energy**

We have measured the activation energies over H-ZSM-5, H-Y zeolite, H-mordenite, silica-alumina, and an unsteamed USY FCC catalyst. The H-Y zeolite showed deactivation at reaction temperatures

above 548 K; no other catalyst showed deactivation in the temperature range of 323 K to 723 K. Arrhenius plots for these catalysts are shown in Figure 13.

The relationship between the strength of the Brønsted acid sites for each catalyst and the activation energy is shown in Figure 14. It is clear from this figure that a relationship exists between the activation energy and the strength of the Brønsted acid sites. This result is consistent with the notion that the strength of the acid sites plays a role in initiating reaction between ammonia and methanol and/or in the adsorption/desorption of reactants and products.

#### **D. Ammonia Order**

Increasing the partial pressure of ammonia generally results in an increase in the turnover frequency for reaction over all catalysts. However, with the H-ZSM-5 catalyst, there is an apparent inhibition effect at higher ammonia pressures as shown in Figure 15. This behavior in NH<sub>3</sub> for H-ZSM-5 contrasts sharply with that shown for H-Y zeolite, and it will require further investigation. An interpretation of these results may be based in the acid strength distribution for the H-ZSM-5 sample used. As shown in Figure 16, the H-ZSM-5 has relatively strong sites, and more importantly has very few sites of weaker strength. Calculations based on adsorption behavior and product molecule basicity indicate that product molecules desorb from the weaker acid sites; consequently, a lower density of weak sites may result in greater susceptibility to ammonia inhibition. This possibility is currently being examined in greater detail.

#### **E. Discussion of Kinetic Results**

The results of our studies suggest that acid characteristics may be the determining feature for initiation of the methylamine synthesis reaction, in view of the different reaction kinetic behavior of the various zeolites and the association of acid features with such behavior. In particular, H-Y zeolites with different Si/Al ratios and different Brønsted acid strengths show different activation energies. At the current time, more zeolite catalysts representing different Brønsted acid strengths are being studied in this regard..

#### **F. Measurement of Thermodynamic Quantities in Methylamine Synthesis**

As outlined in the introduction, one objective of this project is to measure thermodynamic quantities that describe the energetics of reaction pathways of the methylamine synthesis reaction. To this end, microcalorimetry is being employed to measure the heats of adsorption of the reactants and products of the reaction on various catalysts. These catalysts include: H-ZSM-5, H-mordenite, and H-Y zeolite. Representative data are shown schematically in Figure 17 for methanol

and pyridine adsorption on H-ZSM-5. The thermodynamic information obtained from these experiments may be used to quantify the energy profile of the reaction, as shown schematically in Figure 18. Such information, when combined with information obtained from kinetic studies, may eventually yield relationships between thermodynamic and kinetic quantities. The measurements of heats of adsorption also yield information about the association between adsorbate properties (such as gas phase basicity and structure), zeolite acidity and the measured strengths of interaction.

#### IV. Selective Catalytic Reduction of Nitric Oxide

The majority of this report has dealt with our studies of the acidic properties of zeolite catalysts, with a particular application to methylamine synthesis. Our work funded by the Department of Energy has also involved the role of acidity in the selective catalytic reduction of nitric oxide over vanadia/titania catalysts. The quantitative measure of catalyst acidity in these studies was temperature programmed desorption of ammonia. Low surface area materials, comprised of thin films of titania with monolayer amounts of vanadia deposited on the surface, were studied under ultra-high vacuum conditions; and, high surface area catalysts, prepared by impregnation methods, were studied in a conventional flow system. Vacuum TPD spectra provide information about the activation energies for ammonia desorption, while powder TPD studies give information about the enthalpies of desorption. Our measurements from these two approaches gave similar results, indicating that ammonia adsorption was non-activated. The desorption spectra showed contributions from three sites having heats of ammonia desorption of 17, 22 and 26 kcal/mol.

The catalytic properties of these acid sites on vanadia/titania were probed through temperature programmed reaction studies of ammonia preadsorbed on the surface. Studies under ultra-high vacuum conditions were conducted by subsequently adsorbing nitric oxide on the surface followed by heating, whereas studies under flowing conditions were conducted by introducing gaseous nitric oxide in the inert carrier gas prior to heating. In both studies, a dinitrogen formation peak was observed in the temperature programmed reaction spectra. Computer analysis of these spectra showed that the activation energy for reaction of nitric oxide with adsorbed ammonia was approximately equal to 20 kcal/mol. Since the activation energy is essentially the same for reaction of adsorbed ammonia with adsorbed NO (vacuum studies) and with gaseous, or weakly adsorbed NO (powder studies), we suggest that the key step in this process is the activation of ammonia on the surface, e.g., the dehydrogenation of ammonia to  $\text{NH}_x$  species prior to reaction with nitric oxide.

The above results have important implications for industrial application of the selective catalytic reduction of nitric oxide. Since we have measured the acid strength of the sites on vanadia/titania, we can predict the surface coverage by ammonia under industrial reaction conditions,

e.g., 620 K,  $\text{NH}_3/\text{NO} = 1$ , 300 ppm NO. We find that the ammonia coverage is negligible on the weaker sites (17 kcal/mol), indicating that the stronger acid sites are responsible for the selective catalytic reduction of nitric oxide under these conditions. Accordingly, the strategy for preparation of improved catalysts is to prepare materials with stronger acid sites, while maintaining the ability of these sites to activate ammonia.

## V. References

1. Heilen, G., Mercker, H.J., Frank, D., Reck, R.A., and Jaeckh, R., "Amines, Aliphatic," in Ullman's Encyclopedia of Industrial Chemistry, 5th ed. vol. A2, W. Gerhartz ed., p.1, VCH Verlagsgesellschaft, Weinheim FRG (1987).
2. Calkins, W.H., Catal. Rev. Sci. Eng. **26** 347 (1984).
3. Eberly Jr., P.E., J. Phys. Chem. **72**, (1968) 1042 .
4. Cardona-Martinez, N. and Dumesic, J.A., J. Catal. **125**, (1990) 427 .
5. Atkinson, D. and Curthoys, G., J. Chem. Soc. Farad. Trans. I **77**, (1981) 897 .
6. Barthomeuf, D., Mat. Chem. Phys. **17**, (1987) 49 .
7. Barthomeuf, D. and Beaumont, R., J. Catal. **30**, (1973) 288 .
8. Dempsey, E., J. Catal. **33**, (1974) 497 .
9. Dempsey, E., J. Catal. **39**, (1975) 155 .
10. Mikovsky, R.J. and Marshall, J.F., J. Catal. **44**, (1976) 170 .
11. Beagly, B., Dwyer, J., Fitch, F.R., Mann, R. and Walters, J., J. Phys. Chem. **88**, (1984) 1744 .
12. Peters, A.W., J. Phys. Chem. **86**, (1982) 3489 .
13. Peters, A.W., in: Catalytic Materials: Relationship Between Structure and Reactivity, Whyte Jr., T.E., Dalla Betta, R.A., Derouane, E.G. and Bater, R.T.K. (ed.), (American Chemical Society, Washington, D. C., 1984) p201.
14. Haag, W., Fifth Trilateral Meeting on Catalysis, Northwestern University, Evanston, 1991.
15. Forni, L. and Viscardi, C.F., J. Catal. **97**, (1986) 480 .
16. Stach, H., Lohse, U., Thamm, H. and Schirmer, W., Zeolites **6**, (1986) 74.
17. Chen, D., Sharma, S., Bell, V., Hodge, G., Madon, R. and Dumesic, J., Submitted to J. Catal.

18. Biaglow, A.I., Gittleman, C., Gorte, R.J. and Madon, R.J., *J. Catal.* **129**, (1991) 88.
19. Ward, J. and Hansford, R.C., *J. Catal.* **13**, (1969) 364.
20. Ward, J.W., *J. Phys. Chem.* **73**, (1969) 2086.
21. Bielanski, A. and Datka, J., *J. Catal.* **37**, (1975) 383.
22. Jacobs, P.A., Tielen, M. and Uytterhoeven, J.B., *J. Catal.* **50**, (1977) 98.
23. Kapustin, G.I., Kustov, L.M., Glonti, G.O., Brueva, T.R., Borovkov, V.Y., Klyachko, A.L., Rubinstein, A.M. and Kazanskii, V.B., *Kinet. Katal.* **25**, (1984) 1129.
24. Klyachko, A.L., Kapustin, G.I., Brueva, T.R. and Rubinstein, A.M., *Zeolites* **7**, (1987) 119.
25. Mochida, I., A., Y., Fujitsu, H. and Takeshita, K., *J. Catal.* **82**, 313 (1983).
26. Shannon, R.D., Keane Jr., K., Abrams, L., Staley, R.H., Gier, T.E., Corbin, D.R. and Sonnichsen, G.C., *J. Catal.* **114**, 8 (1988).
27. Shannon, R.D., Keane Jr., M., Abrams, L., Staley, R.H., Gier, T.E. and Sonnichsen, G.C., *J. Catal.* **115**, 79 (1989).
28. Keane Jr., M., Sonnichsen, G.C., Abrams, L., Corbin, D.R., Gier, T.E. and Shannon, R.D., *App. Catal.* **32**, 361 (1987).
29. Herrmann, C. and Fetting, F., *App. Catal.* **39**, 213 (1988).
30. Weigert, F., *J. Catal.* **103**, 20 (1987).
31. Segawa, K., Tachibana, H., submitted to *J. Catal.*

## VI. Recent Publications from this Work

Acid Strength of Silica-Supported Oxide Catalysts Studied by Microcalorimetric Measurements of Pyridine Adsorption, Journal of Catalysis, 127, 706 (1991), with N. Cardona-Martinez.

Microcalorimetric Measurements of Basic Molecule Adsorption on Silica and Silica/Alumina, Journal of Catalysis, 128, 23 (1991), with N. Cardona-Martinez.

Microcalorimetric Studies of Zeolite Acidity, accepted for publication in Catalysis Letters, with D. T. Chen, I. Filimonov and S. B. Sharma.

Acidity Studies of Fluid Cracking Catalyst by Microcalorimetry and Infrared Spectroscopy, accepted for publication in the Journal of Catalysis, with D. Chen, S. Sharma, N. Cardona-Martinez, V. A. Bell, G. D. Hodge and R. J. Madon.

Surface Al Coordination in Aluminosilicates Detected with  $^{27}\text{Al}$  NMR, submitted for publication in the Journal of Catalysis, with T. W. Root, Y. Chen, D. T. Chen and N. Cardona-Martinez.

Observation of Brønsted Acid Sites of D-Y Zeolite with Deuterium NMR, accepted for publication in Chemical Physics Letters, with T. J. Gluszak, D. T. Chen, S. B. Sharma and T. W. Root.

Microkinetic Analysis of Isobutane Reactions Catalyzed by Y-Zeolite, 10th International Congress on Catalysis, Budapest, 1991, with J.E. Rekoske, R. J. Madon and L. M. Aparicio.

Temperature Programmed Desorption/Reaction and In Situ Spectroscopic Studies of Vanadia/Titania for Catalytic Reduction of Nitric Oxide, accepted for publication in the Journal of Catalysis, with T. Z. Srnak, B. S. Clausen, E. Törnqvist and N. Topsøe.

Table 1.

Sample	Turnover Frequency (1/s) (603 K, 1:1 NH <sub>3</sub> :CH <sub>3</sub> OH)
Silica-alumina	1.8 x 10 <sup>-4</sup>
H-ZSM-5	1.3 x 10 <sup>-4</sup>
H-Y Zeolite	1.5 x 10 <sup>-4</sup>
H-Mordenite	1.7 x 10 <sup>-4</sup>

## **List of Figures**

Figure 1 - Differential heat plot for pyridine adsorption H-ZSM-5

Figure 2 - Differential heat plot for pyridine adsorption H-Mordenite

Figure 3 - Differential heat plot for pyridine adsorption H-Y zeolite

Figure 4 - Adsorption isotherms at 273 and 473 K on H-Y zeolite

Figure 5 -  $\Delta H$  versus  $\Delta S$  of pyridine adsorption

Figure 6 - TPD spectrum of pyridine from H-ZSM-5

Figure 7 - TPD spectrum of pyridine from H-Mordenite

Figure 8 - IR spectra of pyridine adsorption on H-Y zeolite

Figure 9 - Differential heat plot for pyridine adsorption on H-Y zeolite with different  $\text{Na}^+$  levels

Figure 10 - Differential heat plot for pyridine adsorption on H-ZSM-5 with different  $\text{K}^+$  levels

Figure 11 - Differential heat plot for pyridine adsorption on calcined and fresh H-Mordenite

Figure 12 - Differential heat plot for pyridine adsorption on H-Y FCC catalysts steamed to different extents

Figure 13 - Methylamine synthesis activation energies for different zeolites

Figure 14 - Methylamine synthesis activation energy versus strength of Brønsted sites

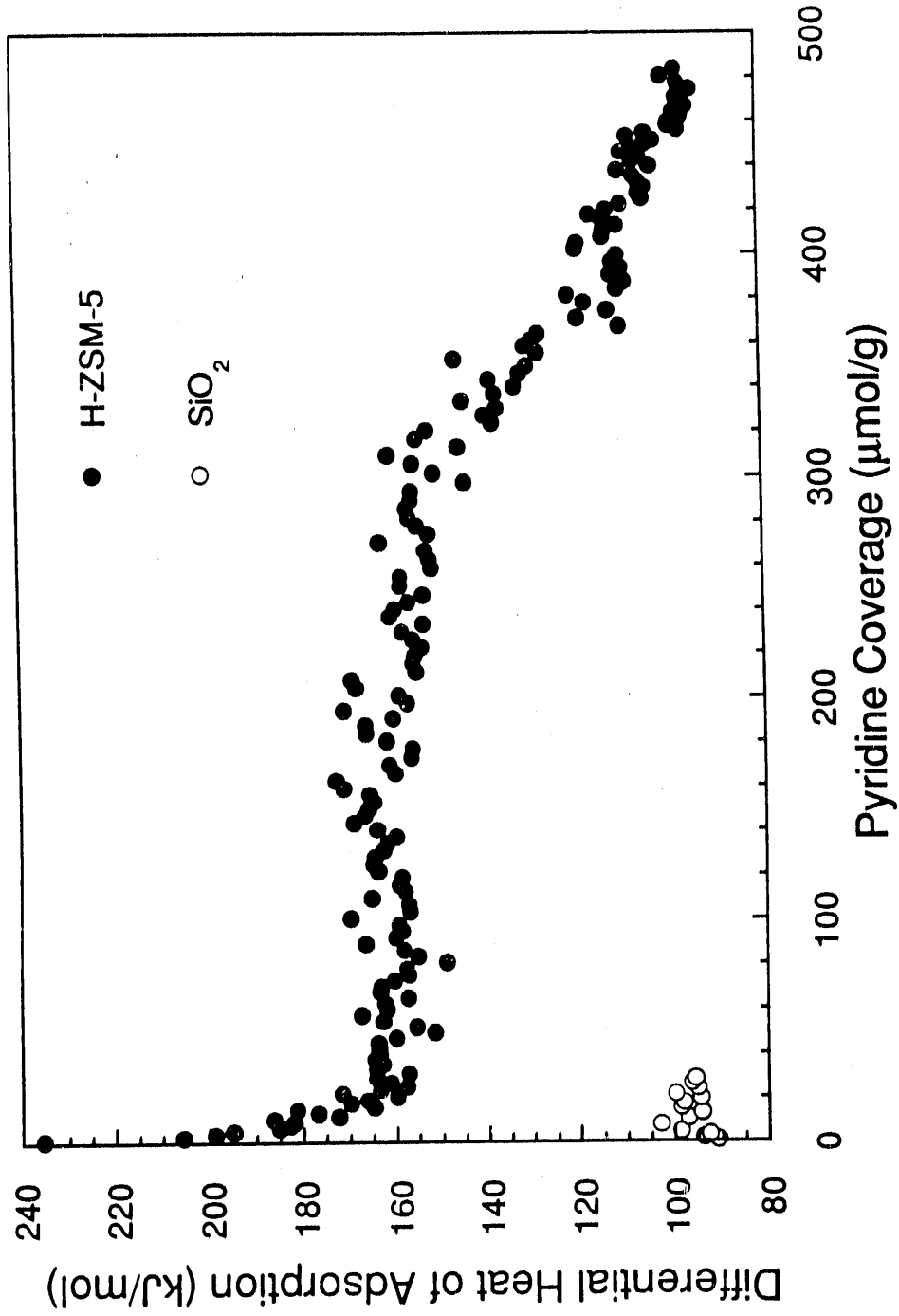
Figure 15 - Methylamine synthesis reaction order in ammonia for H-ZSM-5 and H-Y zeolite

Figure 16 - Different acid strengths for H-ZSM-5 and H-Y zeolite

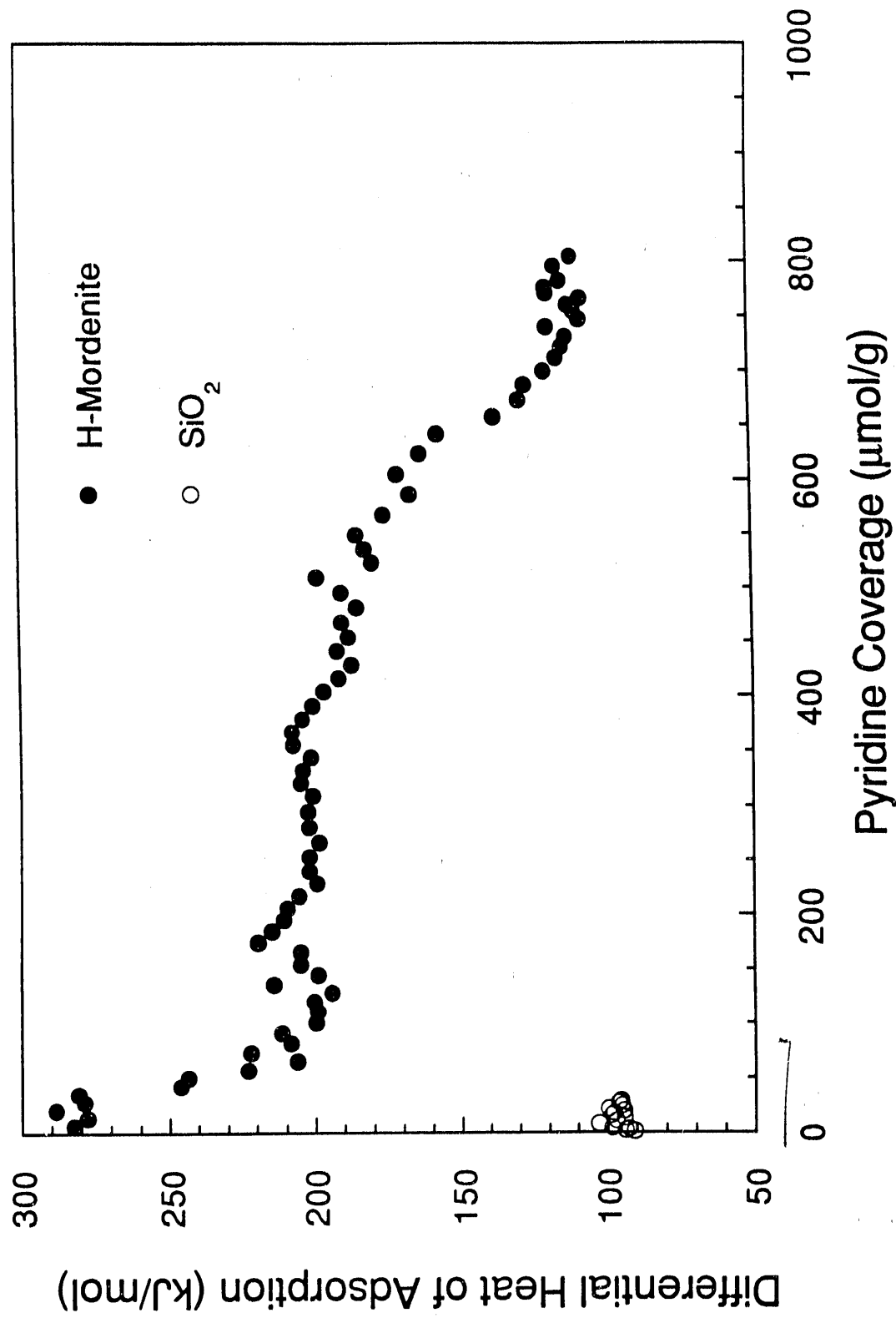
Figure 17 - Differential heats of adsorption for methanol and ammonia on H-ZSM-5

Figure 18 - Schematic energy profile versus reaction coordinate for methylamine synthesis

**Figure 1. Pyridine Adsorption on H-ZSM-5**



**Figure 2. Pyridine Adsorption on H-Mordenite**



**Figure 3. Pyridine Adsorption on H-Y Zeolite**

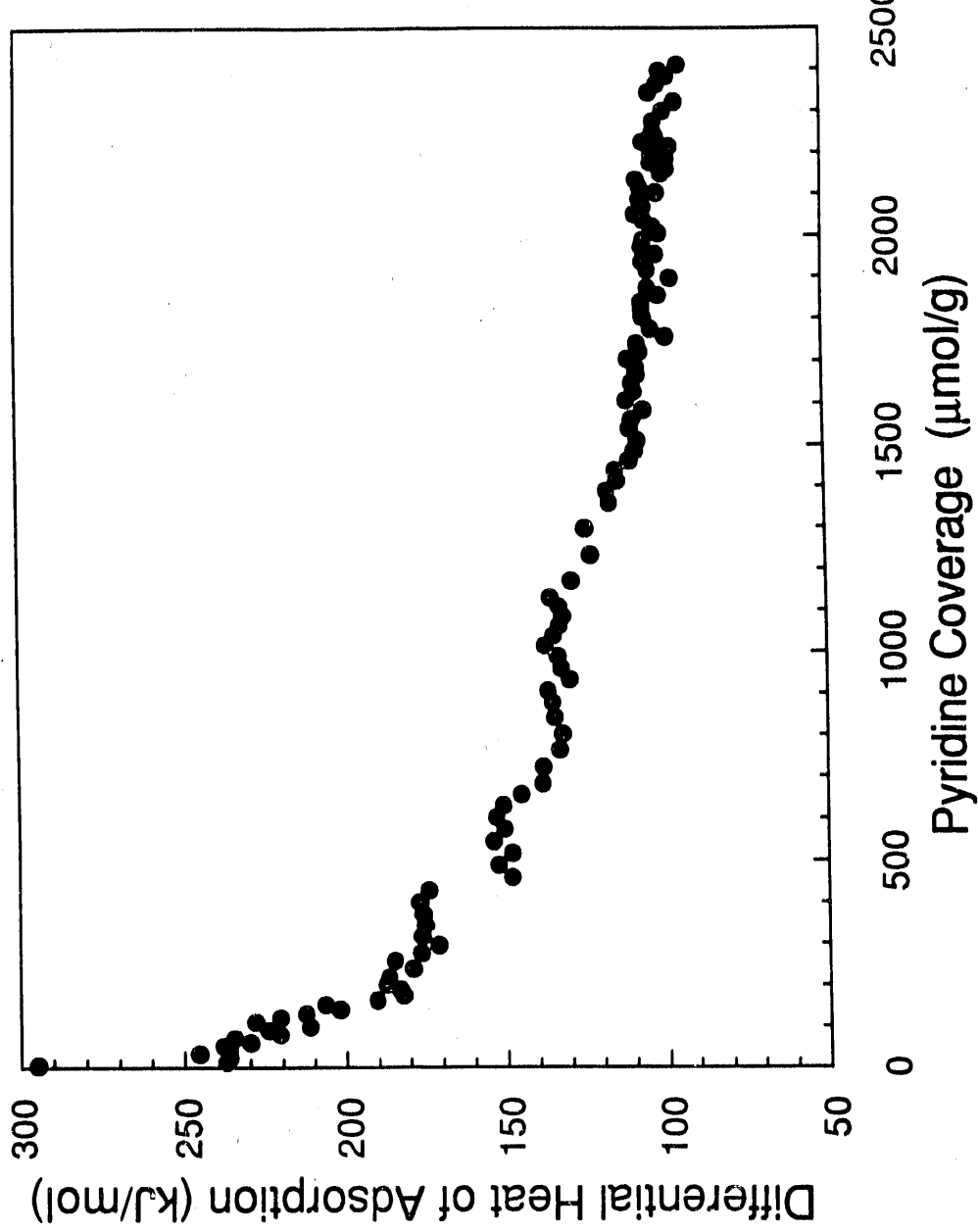


**Figure 4. Pyridine Adsorption Isotherms on H-Y Zeolite**

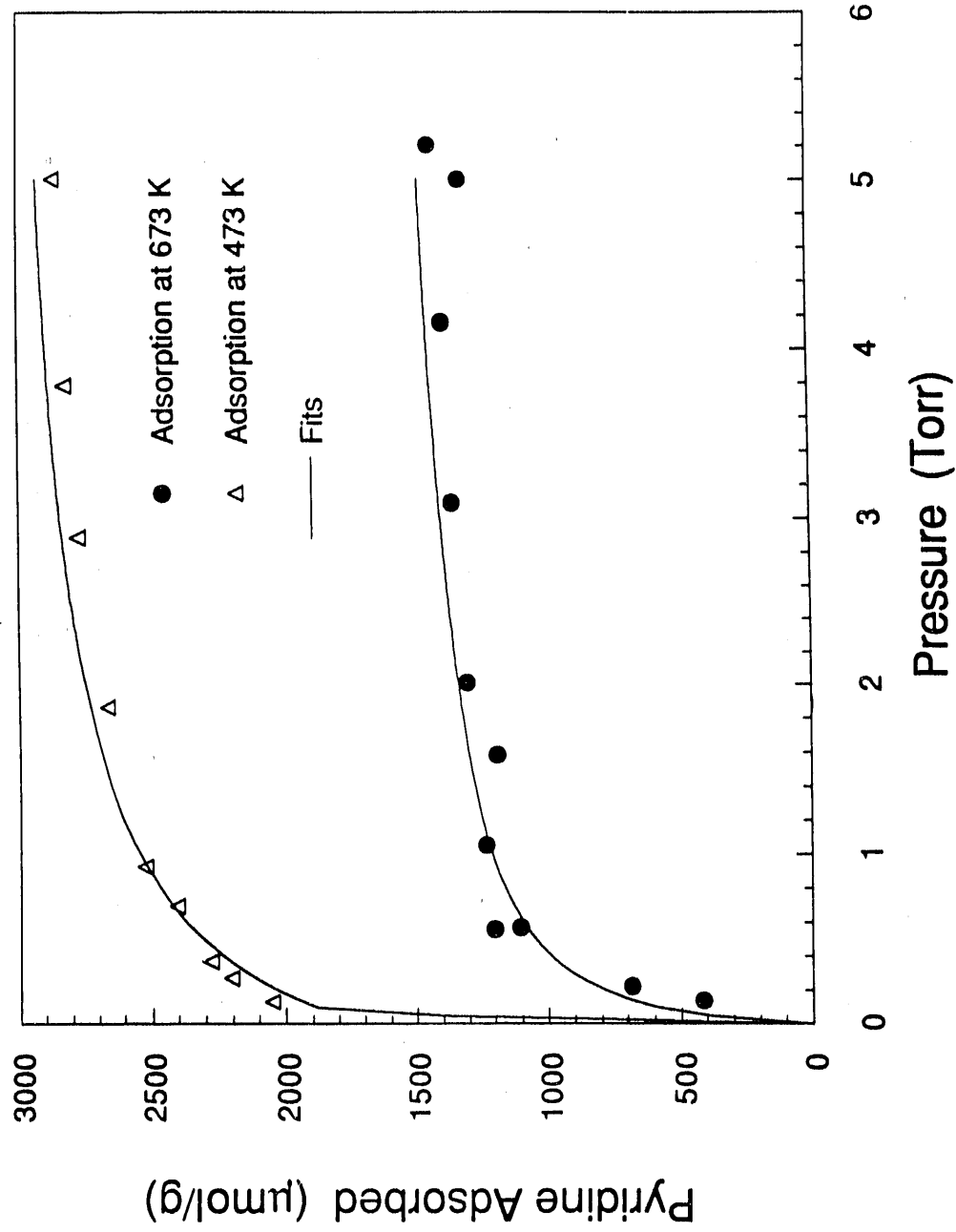


**Figure 5. Entropy of Adsorption versus Heat of Adsorption for Brønsted Sites of Various Catalysts**

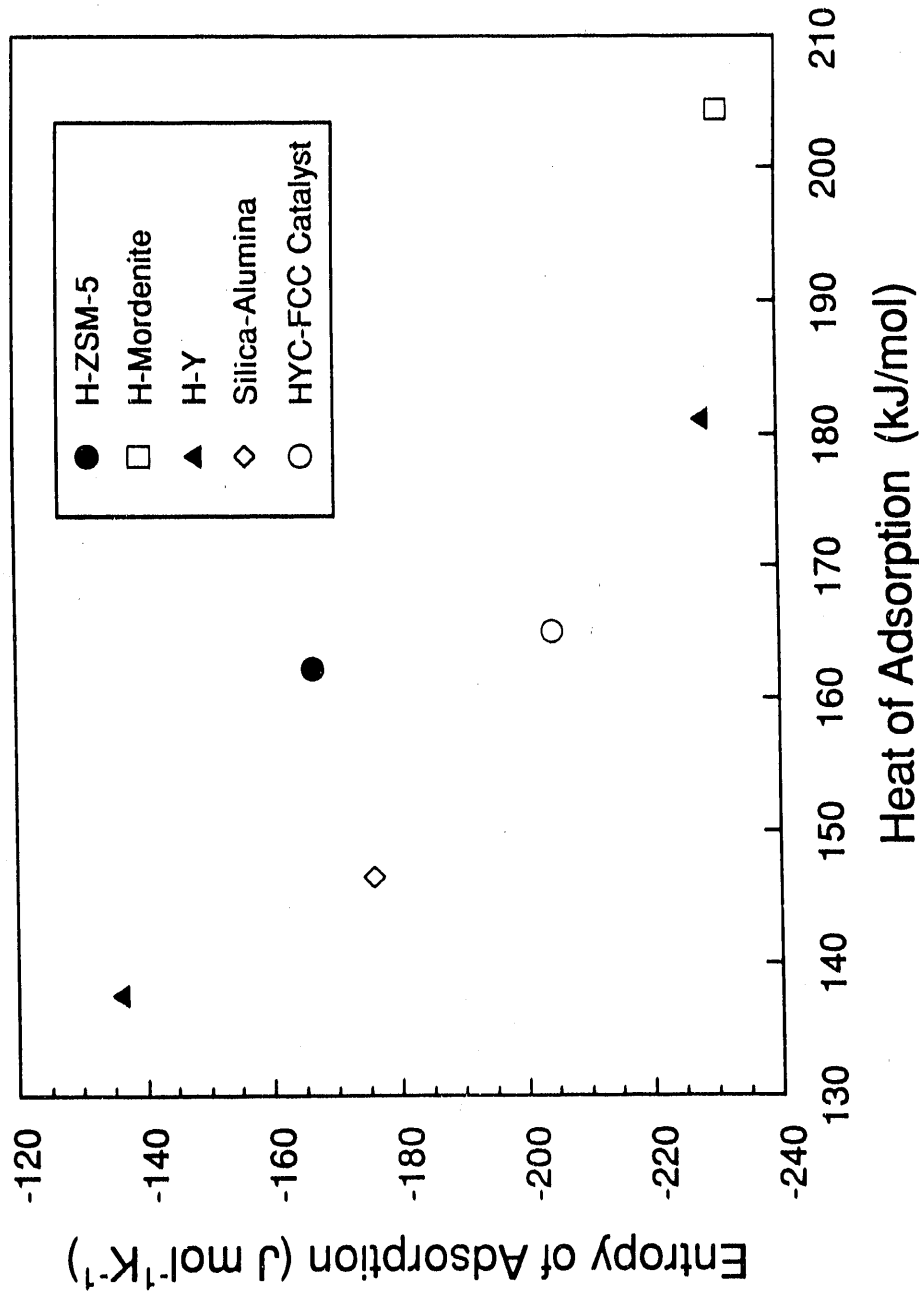


**Figure 6. Pyridine TPD from H-ZSM-5**

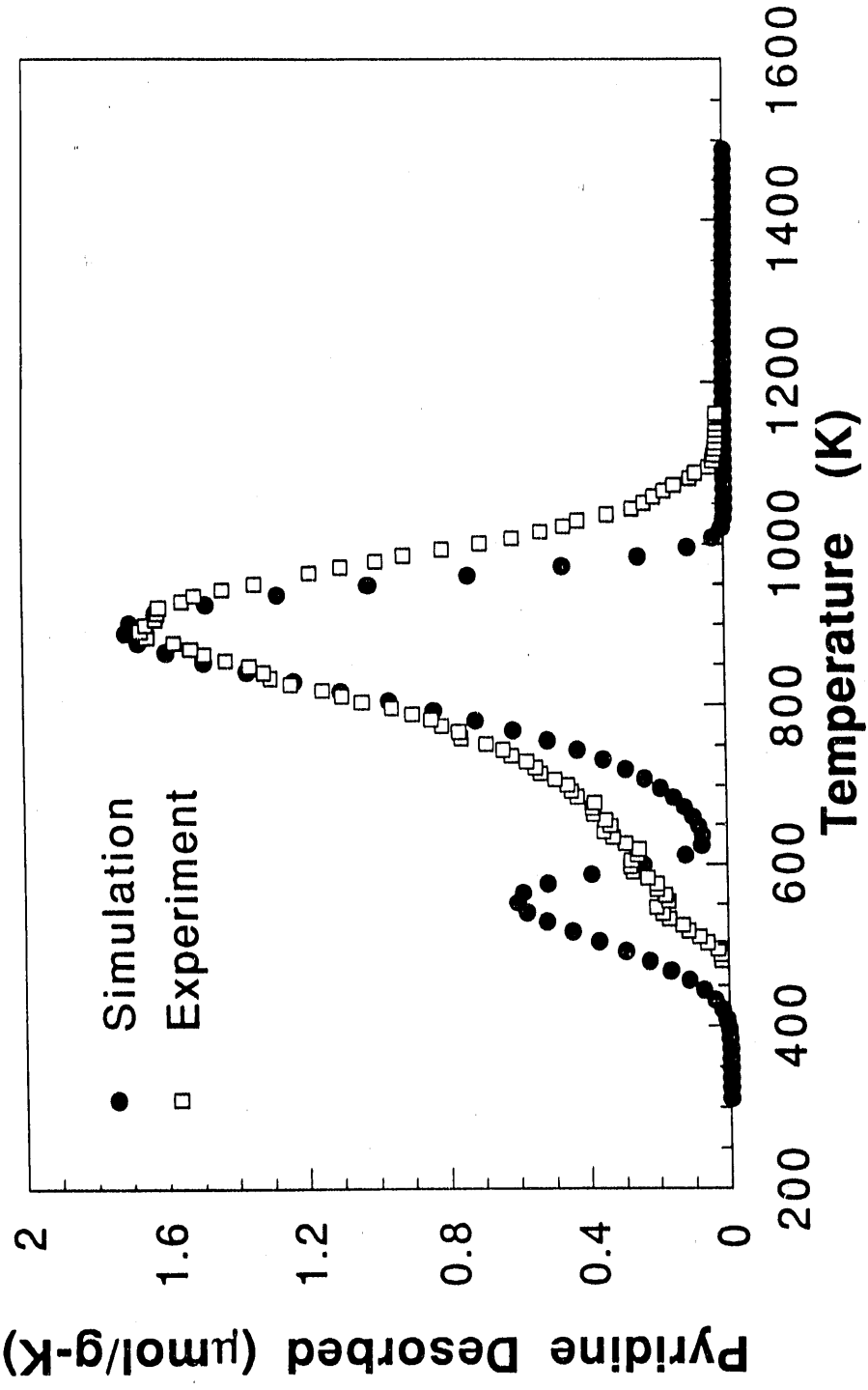


**Figure 7. Pyridine TPD from H-mordenite**

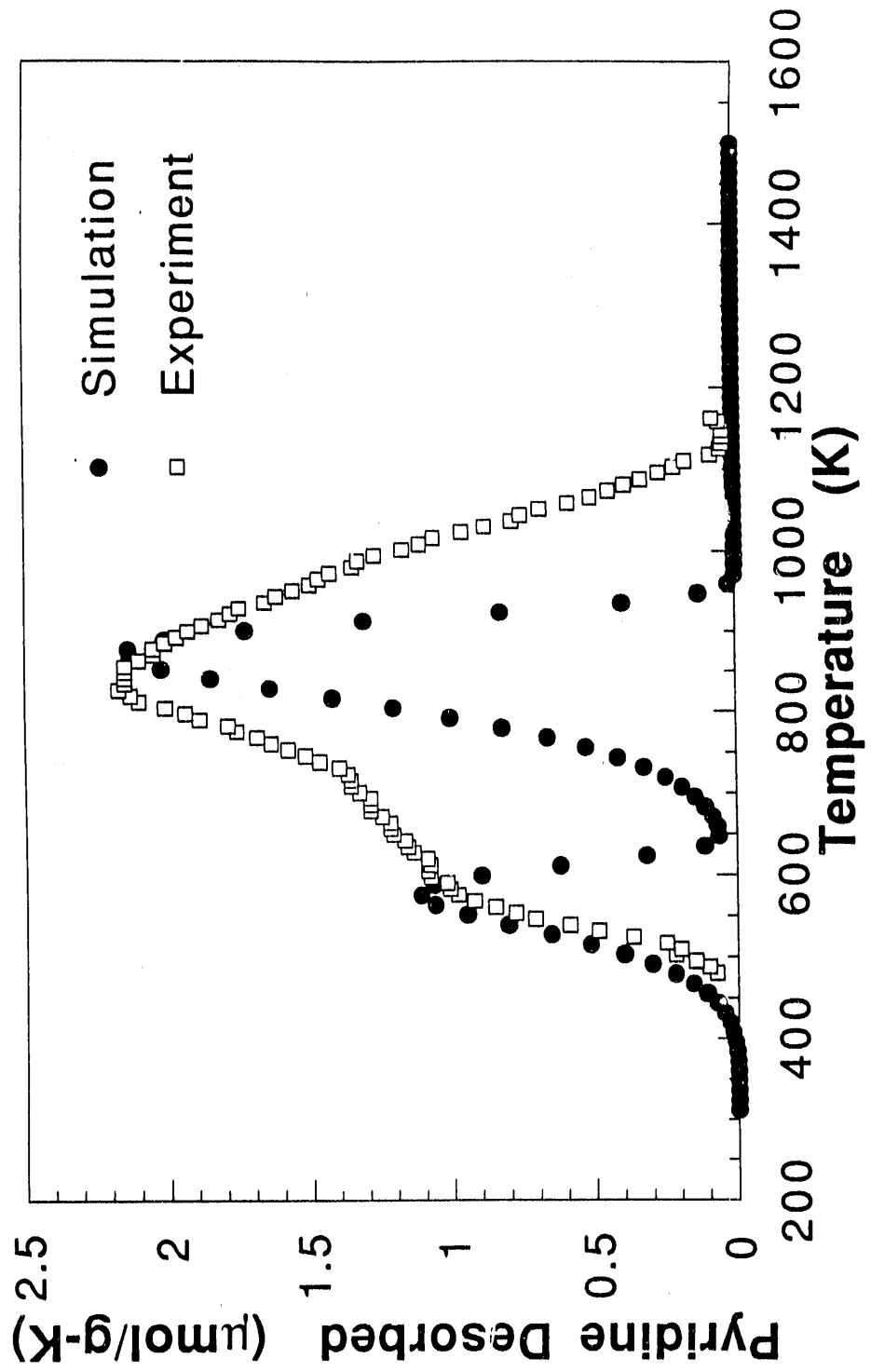
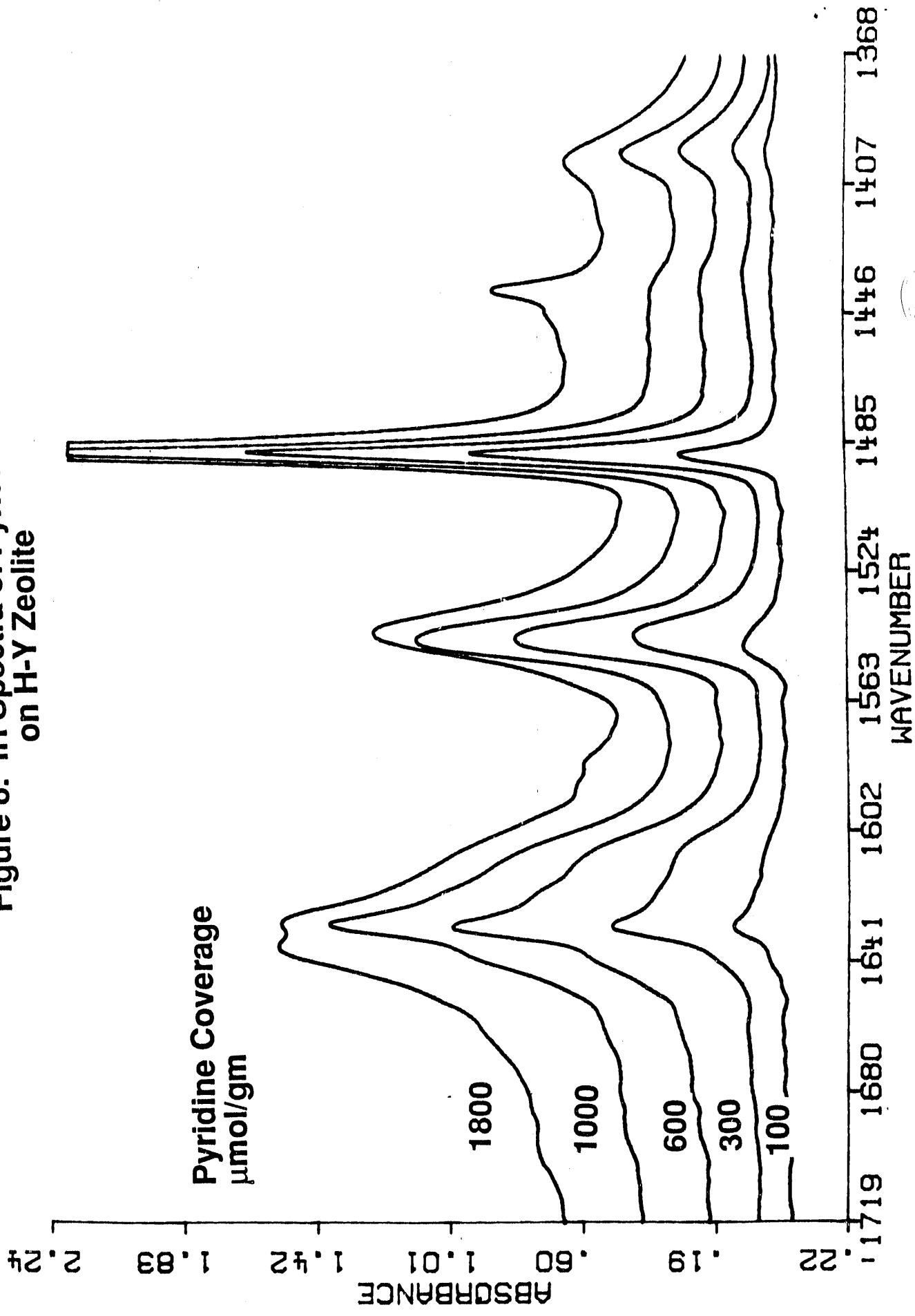
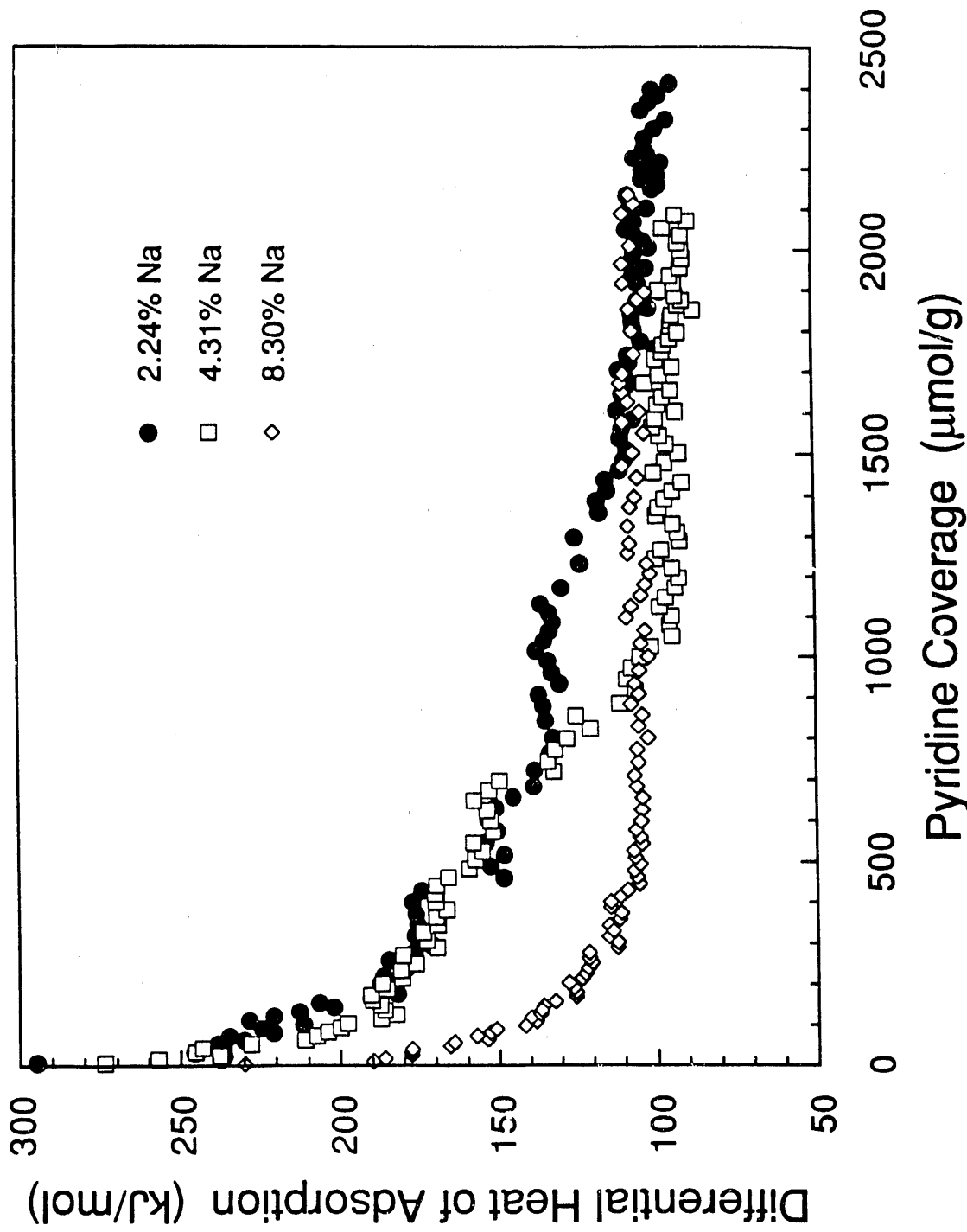


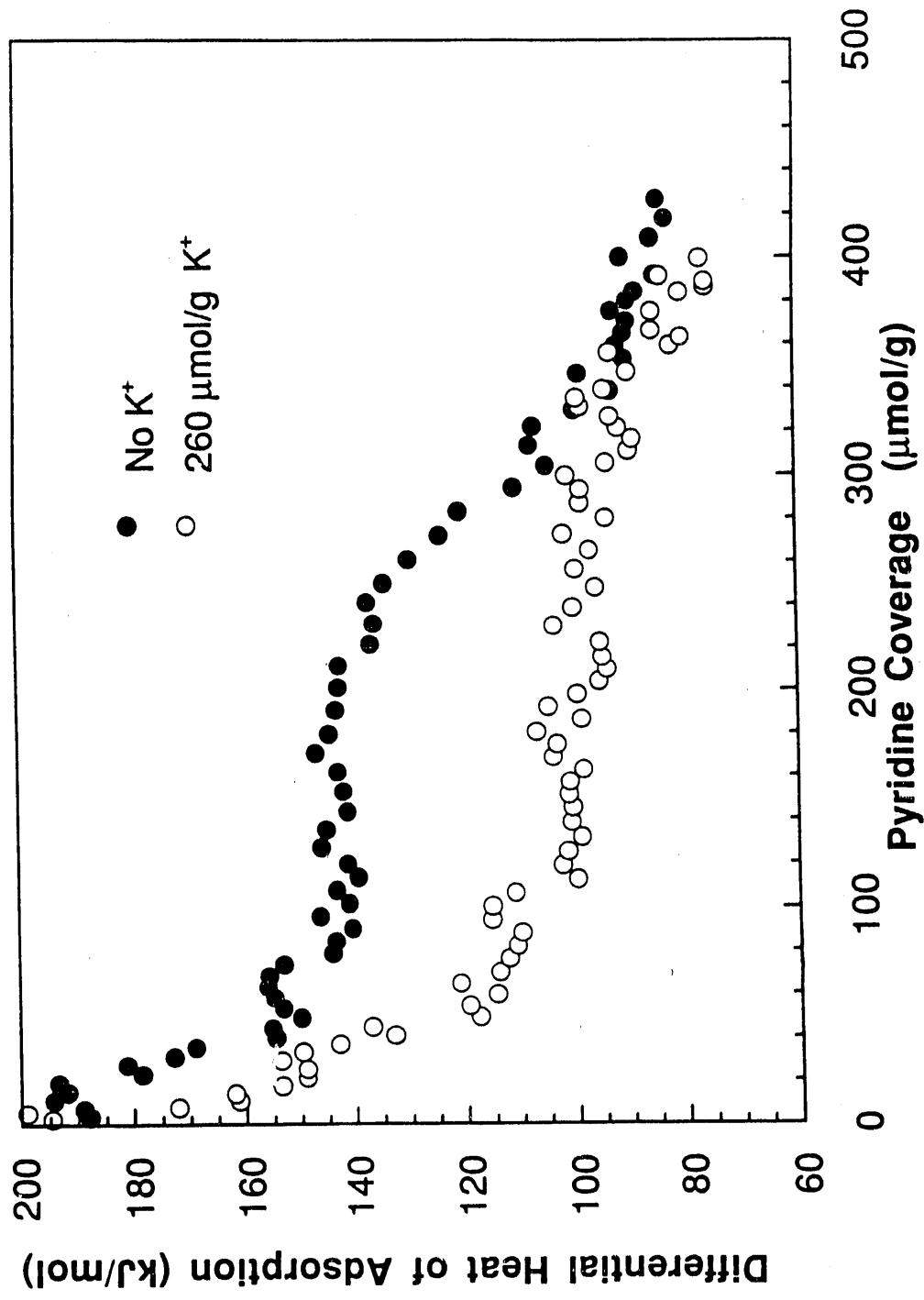
Figure 8. IR Spectra of Pyridine Adsorbed  
on H-Y Zeolite



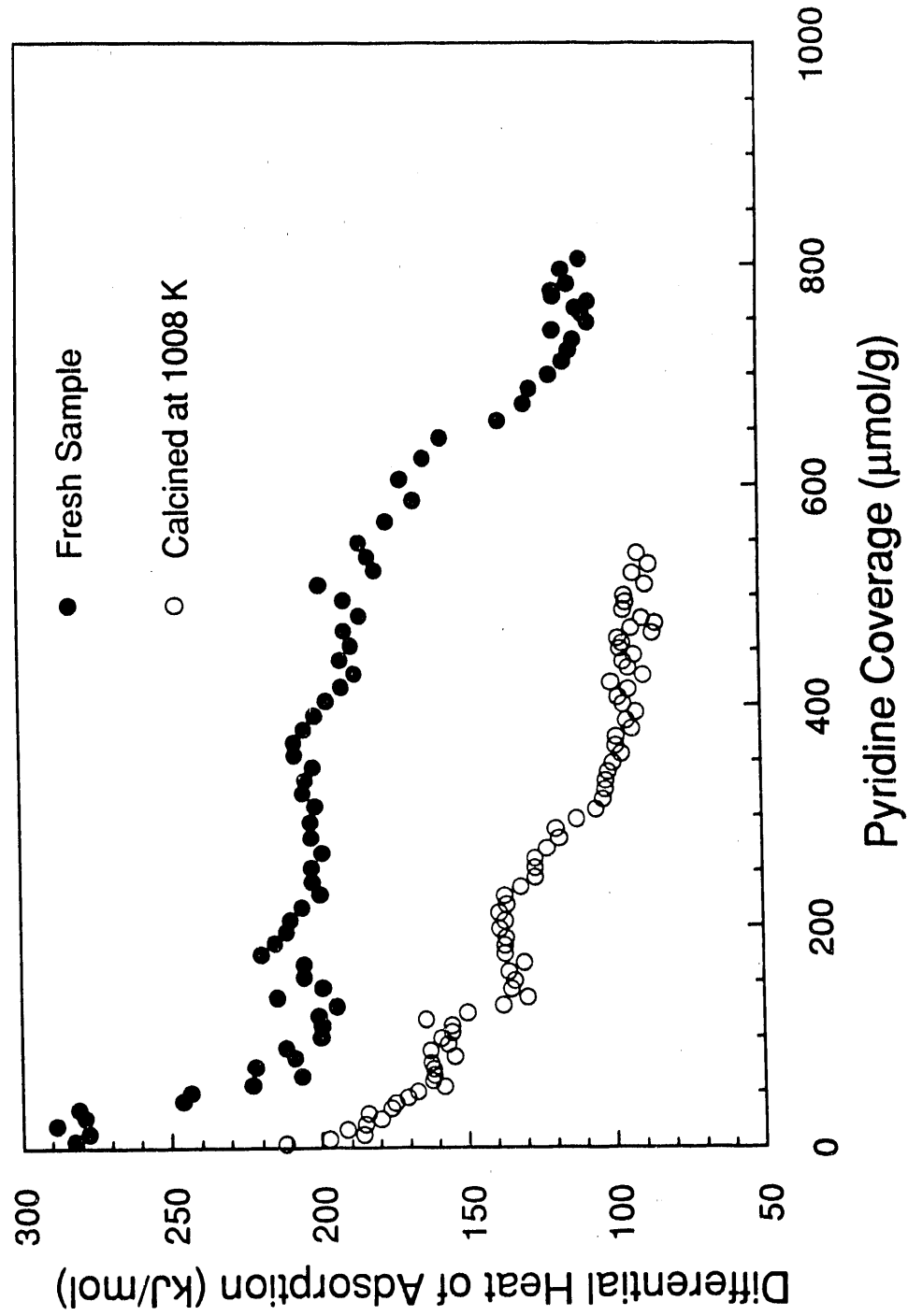
**Figure 9. Pyridine Adsorption on H-Y Zeolites of Varying Na Content**



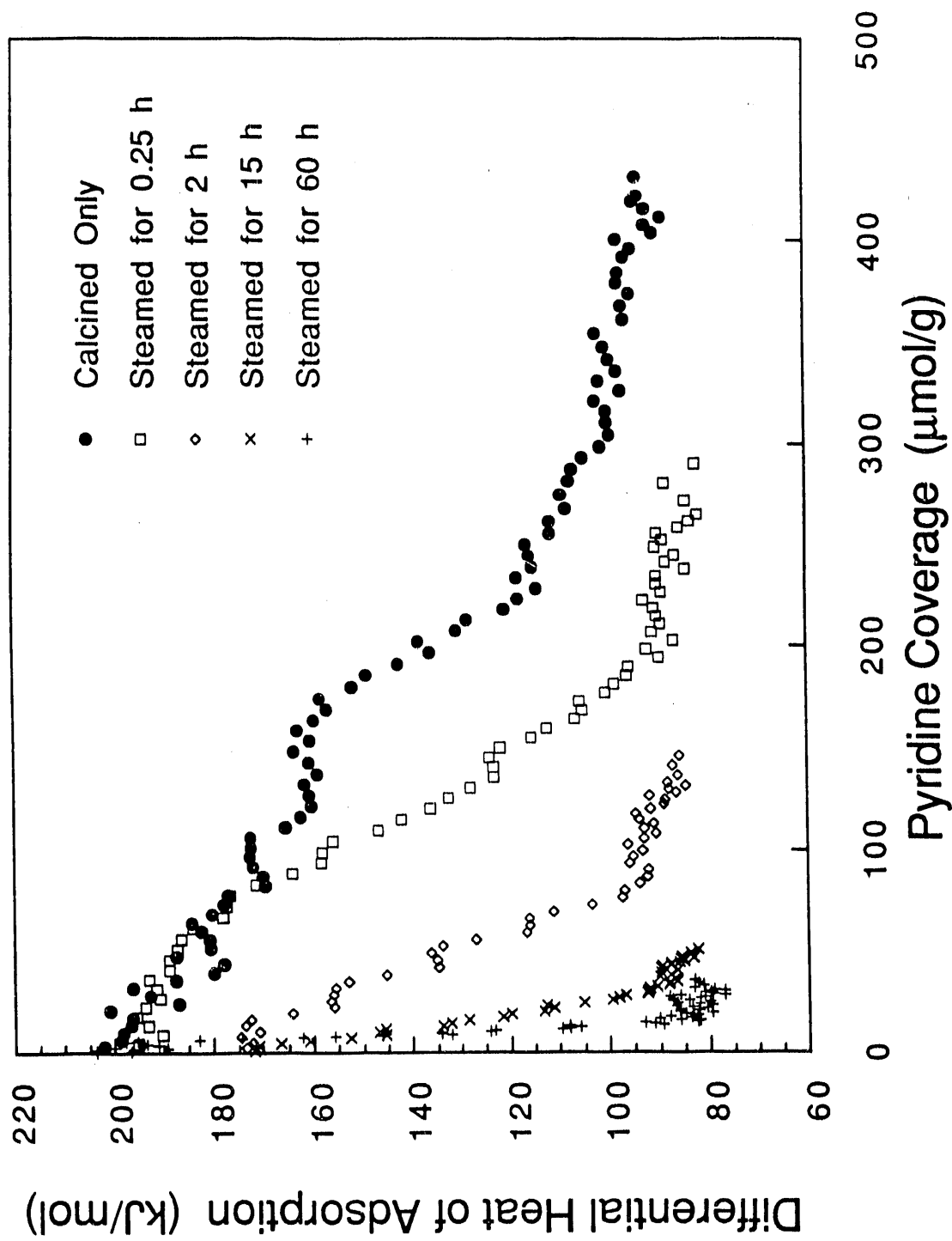
**Figure 10. Pyridine Adsorption on H-ZSM-5 with Varying K<sup>+</sup> Levels**



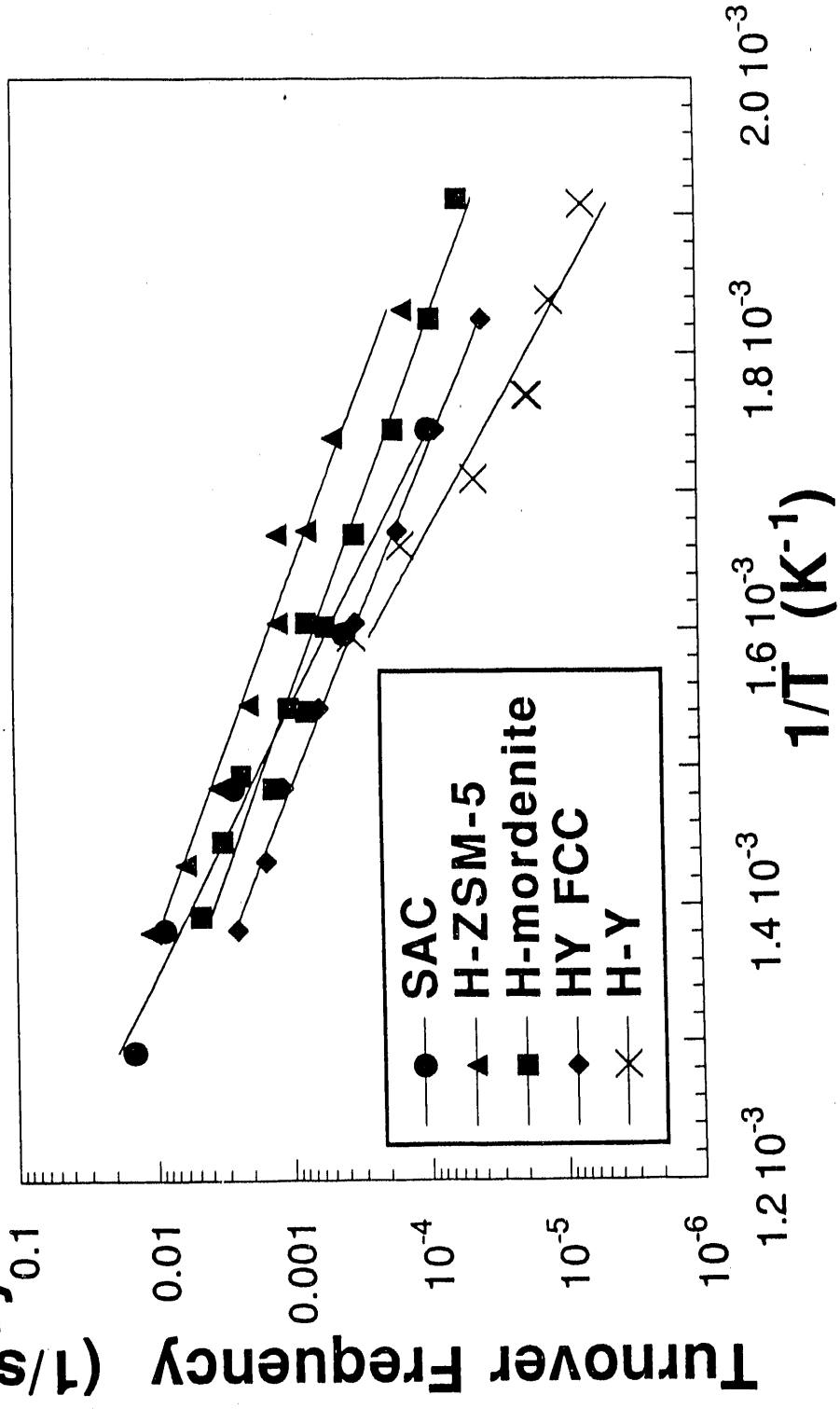
**Figure 11. Pyridine Adsorption on H-Mordenite Before and After High Temperature Calcination**



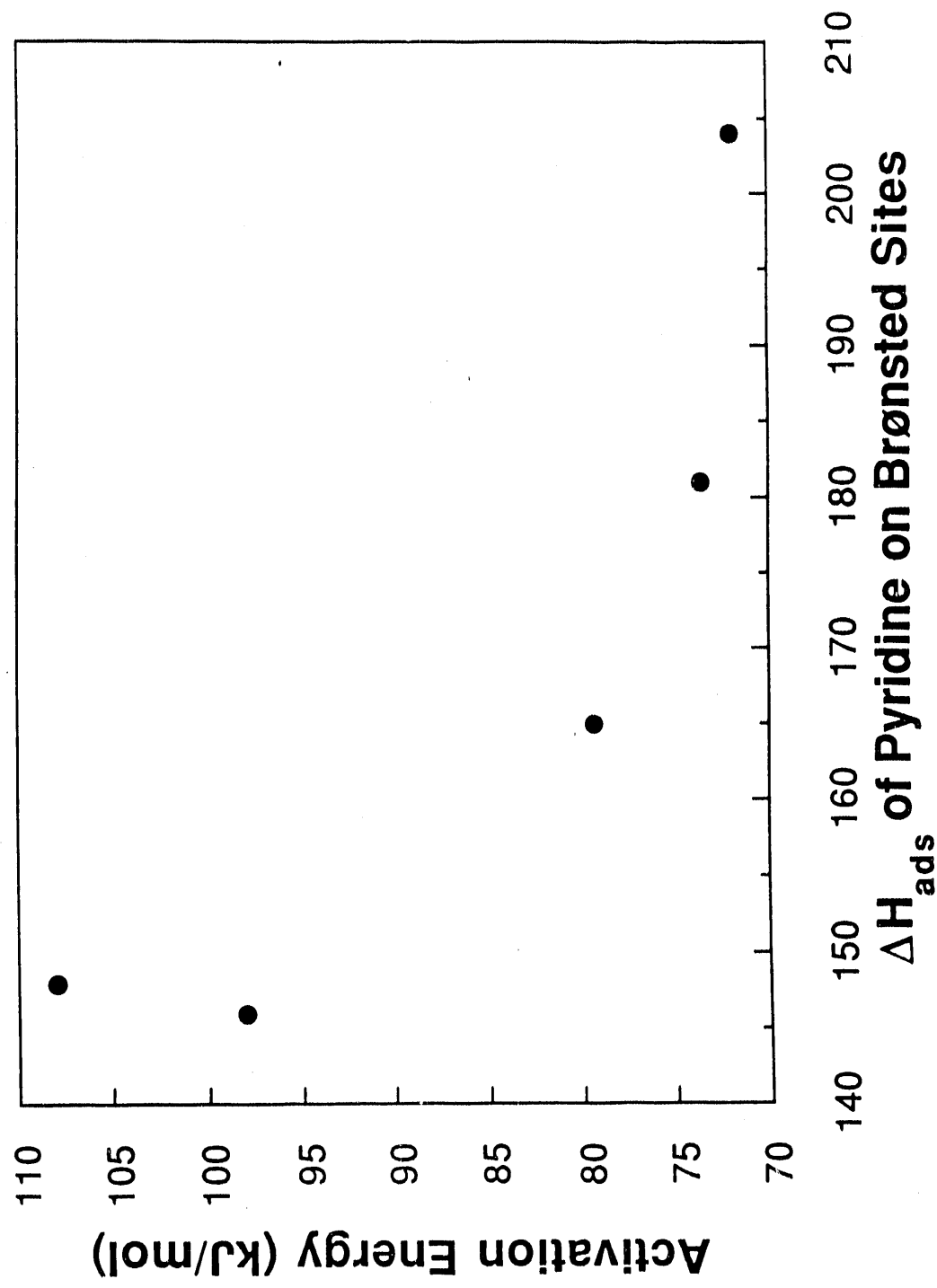
**Figure 12. Pyridine Adsorption on FCC Catalysts Steamed at 1060K**



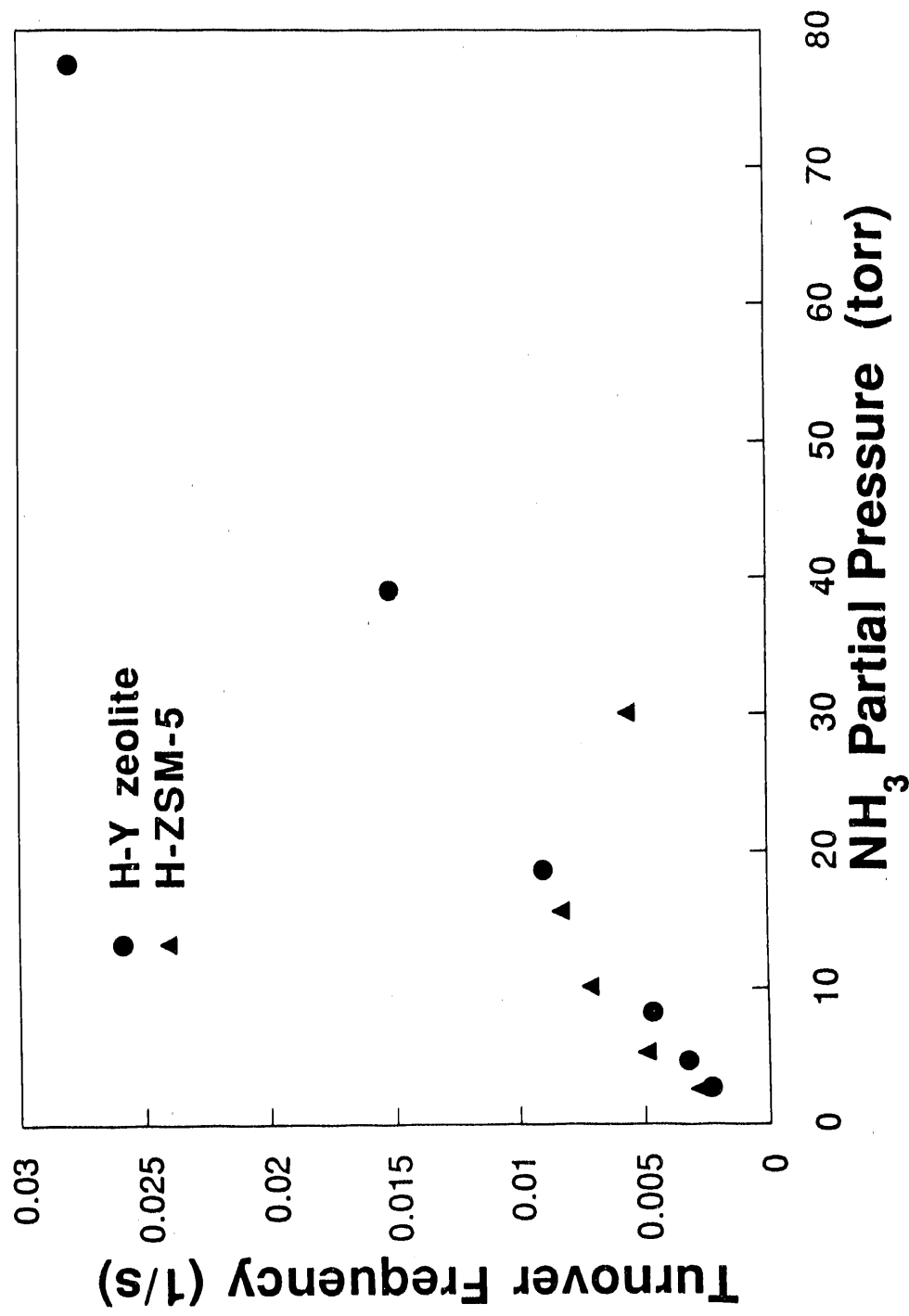
**Figure 13. Arrhenius Plot for Methylamine Synthesis over Various Solid Acid Catalysts**



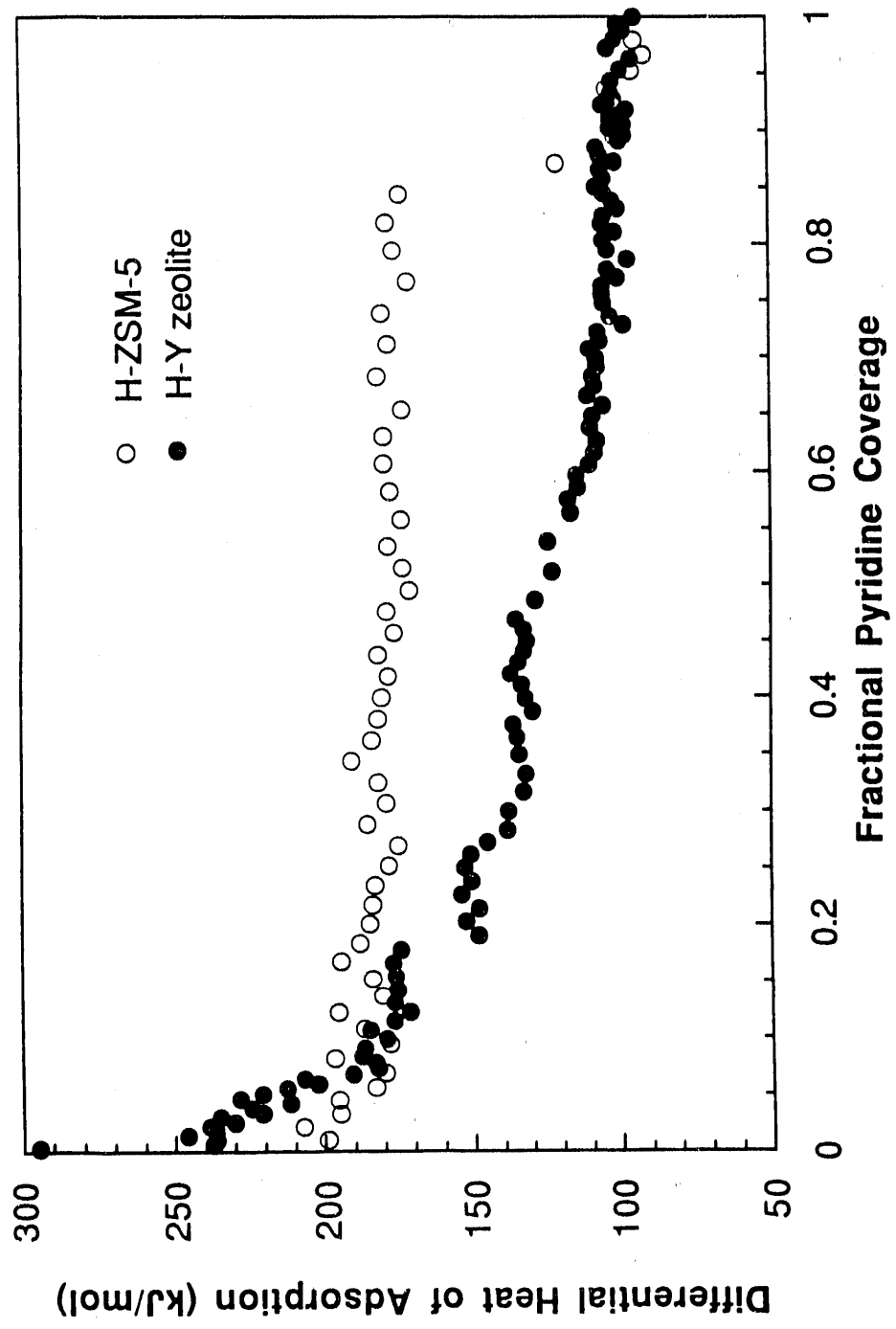
**Figure 14. Activation Energy versus Strength of Brønsted Sites**



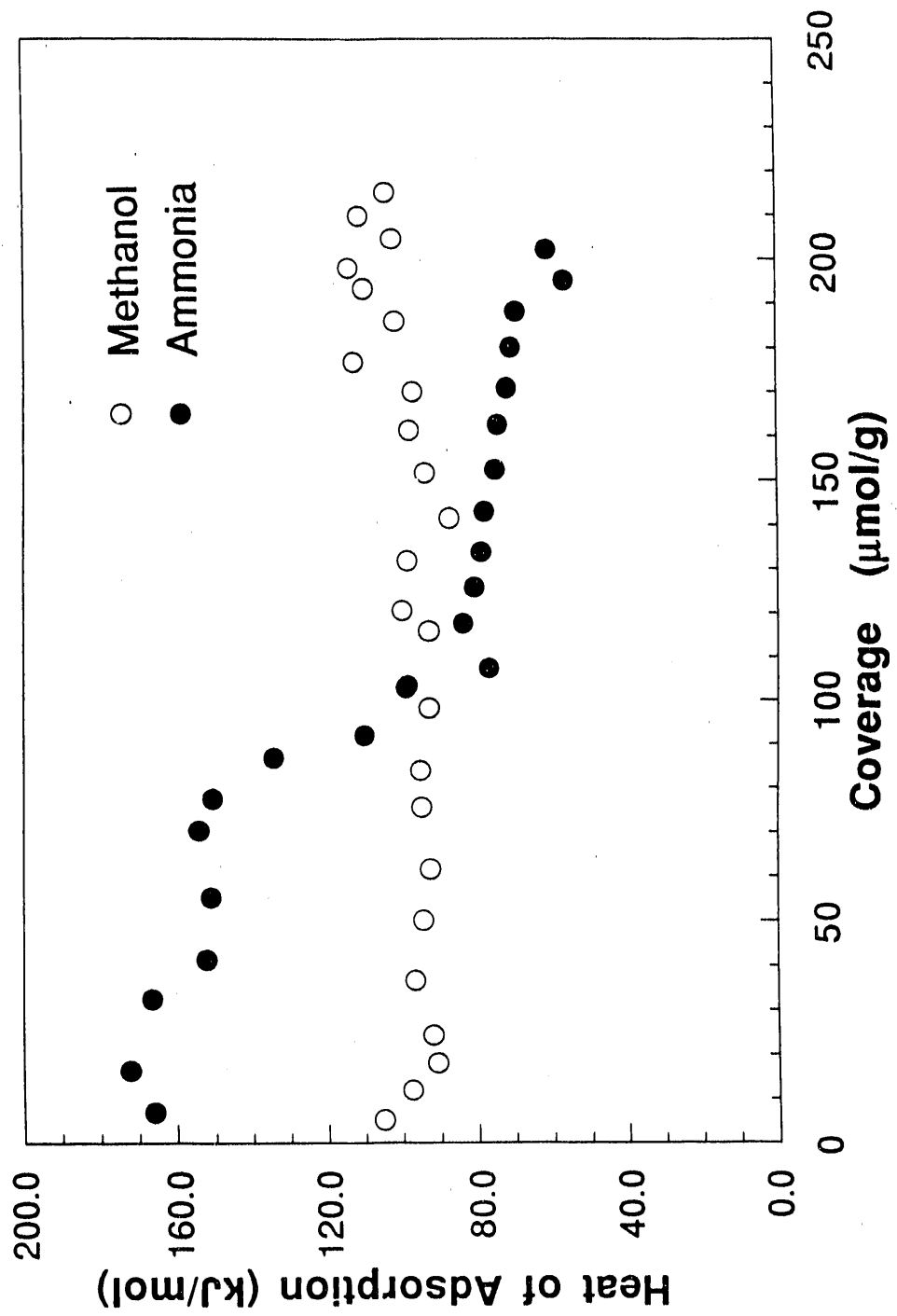
**Figure 15. Ammonia Order Over H-ZSM-5 and H-Y Zeolite**



**Figure 16. Pyridine Adsorption on H-ZSM-5 and H-Y Zeolite**



**Figure 17. Heats of Adsorption of Methanol and Ammonia on H-ZSM-5**



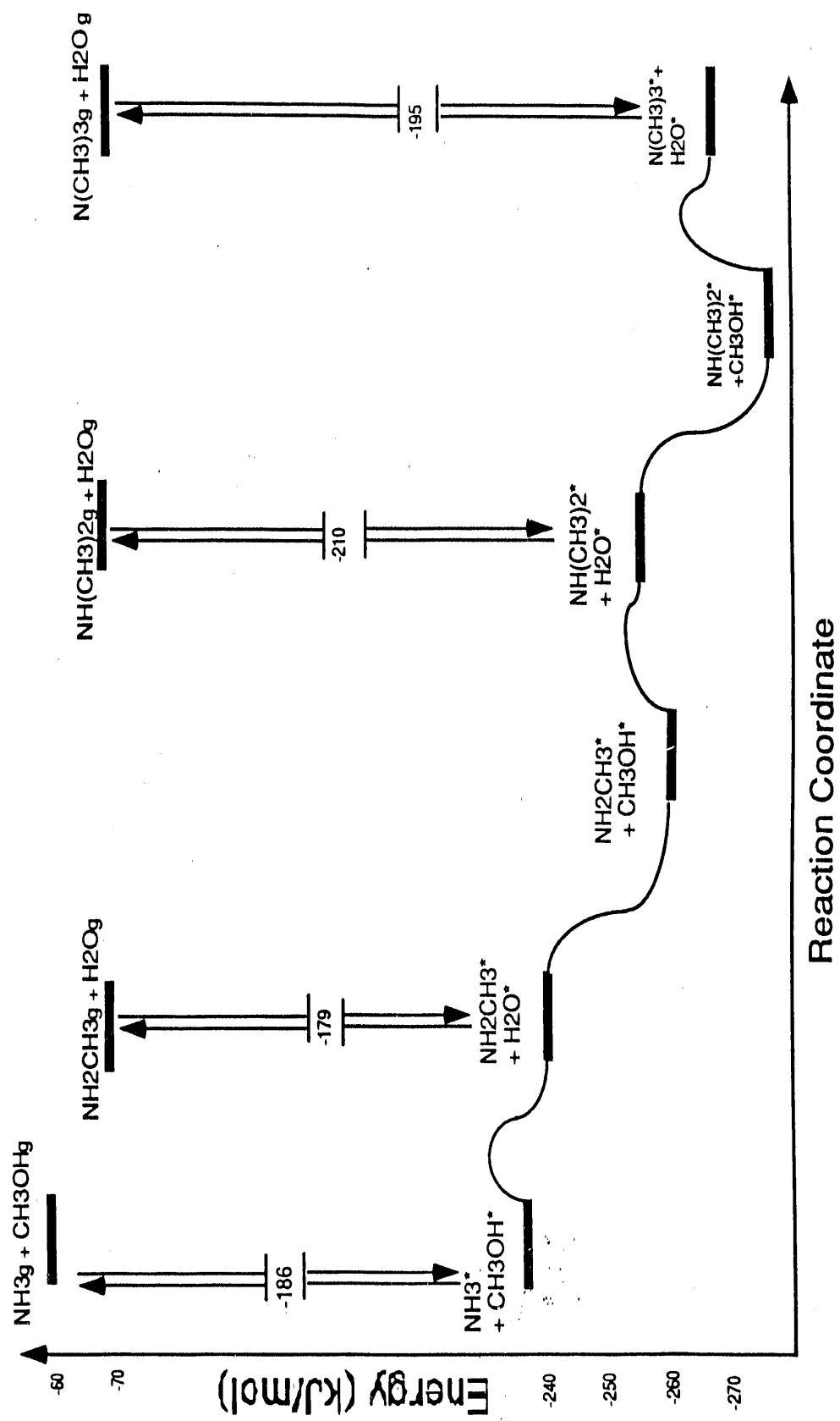


Figure 18. Methylamine Synthesis Energy Profile

END

DATE  
FILMED  
5/18/92

